

## Some geometrical aspects of packing of bent-core molecules in the triclinic smectic- $C_g$ liquid crystals and simple models of the modulated $SmC_{gmod}$ phase

N. V. Madhusudana <sup>\*</sup>

Raman Research Institute, C.V. Raman Avenue, Bengaluru 560080, India



(Received 2 November 2020; accepted 15 January 2021; published 8 February 2021)

Organic compounds with bent-core (BC) molecules usually form the layered smectic liquid crystals with tilted molecules and polarization ( $\mathbf{P}$ ) which lies in the plane of the layer. A few such compounds have been found in which  $\mathbf{P}$  itself tilts out of the plane of the layer, and the medium with general tilt ( $SmC_g$ ) of the molecules has the low chiral triclinic symmetry. We discuss the geometric constraints of molecular packing in this structure to show that projecting groups attached to one of the arms of the BC molecules favors the formation of the  $SmC_g$  phase. We also extend our model for the modulated phases exhibited by BC molecules to show that the stripe structure made of *bilayers* shown by a few BC compounds, which is a signature of  $SmC_g$  layers, is preferentially formed by rotation of the BC molecules about their long axes, rather than about the layer normal. The theoretical results based on the *unified* model which describes *all* the modulated phases exhibited by the BC molecules broadly reflect experimental trends.

DOI: [10.1103/PhysRevE.103.022704](https://doi.org/10.1103/PhysRevE.103.022704)

### I. INTRODUCTION

Smectic liquid crystals (Sm LCs) are condensed matter made of liquid layers of shape anisotropic molecules, with a spatial periodicity only along the layer normal [1]. A large number of mesogenic organic rodlike molecules exhibit such phases. In the  $SmA$  LC, the average orientation direction of the molecular long axes (the director  $\mathbf{n}$ , an apolar unit vector) is along the layer normal, while in the  $SmC$  LC, there is a tilt angle ( $\theta$ ) between the two [1]. The molecules practically freely rotate about their long axes in both LCs. While the nematic ( $N$ ) LC with a pure orientational order is mainly stabilized by excluded volume intermolecular interactions, the layering order in smectic LCs essentially results from biphilicity of the molecules, which have strongly polarizable aromatic cores, with more flexible and weakly polarizable aliphatic chains at one or both ends. As we have argued earlier [2,3], off-axis lateral dipolar groups of the molecules lead to the tilting of the freely rotating molecules in the layers of  $SmC$  LC, which has the monoclinic  $C_2$  symmetry, with a mirror in the tilt plane. In principle, boardlike biaxial molecules which do not freely rotate even about their longest axes can lead to the formation of *biaxial N* and  $SmA$  LCs [1]. In the case of  $SmC$  LCs, such molecules can give rise to a *general* tilting of the *nonrotating* molecules, with *none* of their principal axes (for example, those corresponding to the moments of inertia) oriented along any direction in the plane of the layers in the resulting  $SmC_g$  phase. The structure has the *triclinic chiral* symmetry  $C_1$ , and if the molecules are not chiral, both right-handed and left-handed layers can form with equal probability. However, compounds made of boardlike molecules with the required anisotropies are usually not mesogenic.

Compounds made of rods with *bent cores* (BCs, Fig. 1) have *shape polarity* in addition to biaxiality. A large number of such compounds exhibit Sm LCs, the nonrotating BC molecules packing with a polar order ( $\mathbf{P}$ ), with their long axes tilted most often in the plane orthogonal to  $\mathbf{P}$ , and the layer structure of the resulting  $B_2$  LCs is described by the symbol  $SmCP$  [4]. The tilt angle  $\theta$  of the long axis (of length  $l$ ) of the BC molecule reduces the layer spacing to  $d = l\cos\theta$ . The structure with the *molecular plane* containing the long axis and the two bent arms being *orthogonal* to the *tilt plane* defined by the long axis and the layer normal  $\zeta$  has the monoclinic  $C_2$  symmetry (Fig. 1). The *layers* become chiral, whose sense depends on the direction of tilt about  $\mathbf{P}$ . Many such compounds have *moderate* polarization  $\mathbf{P}$ , and exhibit *stripes* formed by splayed polarization ( $\text{div}\mathbf{P}$ ) in the layers. The stripe width  $w$  is in the range of 10–100 s of *nm*, and the structure of the resulting  $B_7$  LC has two-dimensional periodicity [5]. The  $B_7$  phase usually separates from the isotropic phase at a transition temperature, the stripe width  $w$  increasing as the temperature is lowered, and undergoes a weak first order transition to the  $B_2$  ( $SmCP$ ) phase without stripes at some lower temperature. Typical BC molecules have several phenyl rings, connected by at least one, and usually more, ester linkage groups, which provide structural *flexibility* to the molecules because of relatively easy rotational freedom about the single bonds. The molecules exhibit conformational variety, with a substantial ( $\sim 10$ – $20\%$ ) fraction of the molecules in excited state (ES) conformations with smaller bend angles compared to the ground state (GS) more bent molecules. We [6,7] have recently argued that the ES conformers can rotate freely about their long axes, and can aggregate to gain rotational entropy to form domains without any polarization. The  $\mathbf{P}$  vector of the GS molecules aligns perpendicular to the interface formed between the two domains. The positive polarization energy cost of this arrangement is overcome by the allowed  $\text{div}\mathbf{P}$

<sup>\*</sup>nvmadhu@rri.res.in

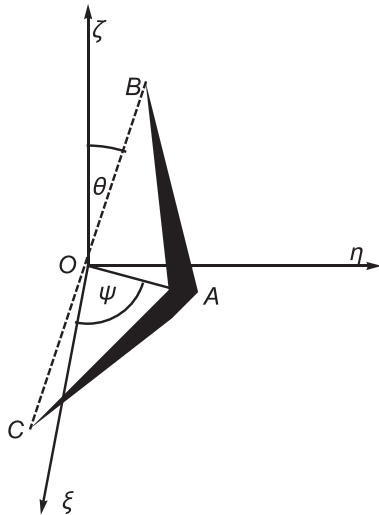


FIG. 1. Orientation of a bent-core molecule  $ABC$  in a  $SmC_g$  layer whose normal is along the  $\zeta$  axis. The long axis  $BC$  which lies in the  $\eta\zeta$  plane makes the tilt angle  $\theta$  with  $\zeta$ . The arrow axis  $OA$  makes the angle  $\psi$  with the  $\xi$  axis. In the  $SmCP$  layer of the  $B_2$  liquid crystal,  $\psi = 0$ .

distortion. We have developed a phenomenological theory of the  $B_7$  phase on the basis of this argument [6,7], and shown that the increase of  $w$  as the temperature is reduced, the effect of external electric field on the structure, the  $B_7$ – $B_2$  transition, the increase in  $w$  with time as the sample deteriorates, etc., predicted by the model are in close agreement with the experimentally measured trends.

In favorable cases the biaxiality of the BC molecules can be expected to give rise to the  $SmC_g$  phase described above. This “double tilted” structure has been described using two different (broadly equivalent) schemes. In one, starting with the  $SmCP$  structure mentioned above, the  $\mathbf{P}$  vector leans (or tips) by some angle in the molecular plane, and away from the plane of the layer [8]. In this scheme, the net tilt angle made by the long axis itself changes after the second operation, changing the layer spacing, which depends on both angles. We find it convenient to follow the scheme in which in the second operation the arrow axis rotates *about* the long axis of the molecule by some angle  $\psi$ , and the tilt angle  $\theta$  of the long axis remains unaltered [9]. In either case,  $\mathbf{P}$  is no longer in the layer plane, but has a component along the layer normal (Fig. 1). The resulting structure has the triclinic  $C_1$  symmetry corresponding to the  $SmC_g$  LC described earlier. The structure is again chiral, except in the special case of  $\psi = \pi/2$  rad, in which case the molecular and tilt planes are coplanar, and the resulting monoclinic  $C_2$  symmetry is achiral. General phenomenological models have been developed to describe the LC, including different possible mutual arrangements of the orientations of the BC molecules between neighboring layers [10,11]. In one molecular description, the BC molecule is idealized as a filled isosceles triangle with built-in wedge shape [12]. Based on calculations of excluded volume between such molecules, it is argued that the  $SmC_g$  structure leads to bending of the layers, caused by a splay distortion of the component of  $\mathbf{P}$  along the layer normal. A

detailed molecular theory of BC molecules with a dipole on each arm, and taking into account the excluded volume, dispersion, and dipolar interactions, has been developed to show that the  $SmC_g$  phase with  $\psi = 90^\circ$  can result if the dipole moment is *small*, and the bend angle of the molecule is relatively *large* [13]. There have also been many reports of observation of the  $SmC_g$  phase, based on different types of experimental results. In the following we summarize only those results which are unambiguous.

Detailed optical mapping of the spatial dependence of the dielectric tensor between  $2\pi$  walls of  $\mathbf{P}$  in a free standing *single smectic layer* of the BC compound NORABOW (Fig. 2) has been used to measure both the tilt angle  $\theta$  ( $\sim 40^\circ$ ) of the long axis and the rotation angle  $\psi$  of the arrow head ( $\sim 19^\circ$ ) [9]. This shows that the  $SmC_g$  results from *in-layer molecular interactions*. Similar studies on a stack of four or six layers are consistent with the above result [14]. Interestingly, if the symmetric molecules do *not* have the OH-group substitutions on the two arms, the compound exhibits *only* a simple  $B_2$  phase. Optical studies on the influence of a lateral DC electric field on thick ( $\sim 1 \mu\text{m}$ ) free standing films of a compound made of *asymmetric* BC molecules with the bulky  $\text{Si}(\text{CH}_3)_2\text{-Si}(\text{CH}_3)_2\text{-Si}(\text{CH}_3)_3$  group only at one end have been used to argue that it forms a low temperature phase in which the molecular plane lies in the tilt plane [15]. The tilt angle  $\theta \approx 20^\circ$ , and  $\psi = 90^\circ$ , and the structure has the achiral  $C_2$  symmetry (Fig. 1). Asymmetric BC molecules with different chemical structures and/or physical dimensions of the two arms are natural candidates for the occurrence of the  $SmC_g$  phase.

X-ray studies are routinely employed to measure the tilt angle  $\theta$  using the layer spacing  $d$ , and to analyze the two-dimensional (2D) lattice which results from the stripe structure of the  $B_7$  phase. In some compounds, apart from the strong scattering corresponding to  $d$ , a weak Bragg spot corresponding to the *bilayer* spacing  $2d$  is seen as well. If the two arms have different chemical structures but similar physical dimensions, in principle bilayers which can be detected by the normal x-ray scattering can result even in  $B_2$  LCs with  $\psi = 0$ . This condition is not met usually, and molecules which have asymmetries in the physical dimensions of the two arms are more likely to exhibit the bilayer scattering. These molecules can in general exhibit  $SmC_{g2}$  phases, the symbol  $g2$  indicating  $SmC_g$  with a bilayer structure. This is possible only if the  $\psi$  rotations in neighboring layers are correlated suitably, depending on their clinality. Detailed x-ray and electro-optic studies on a homologous series of compounds with *symmetric* BC molecules  $E_{Bm}$  (Fig. 3) have shown that bilayer structures arise in a few homologs with intermediate chain lengths with 10–14 carbon atoms ( $m$ ), while both shorter and longer molecules outside this range give rise to only monolayer structures [16]. Indeed the bilayer structures exhibit two-dimensional periodicities, and are bilayer analogs of the  $B_7$  phase mentioned above.

Electro-optic studies on  $E_{Bm}$  show that above a *threshold* electric field the polarization reverses with that of the field by a *rotation* of molecules about the *long axes*, while for homologs with  $m \geq 14$  above a *second threshold*, the process involves a *cone rotation* about the *layer normal*. It is noteworthy that in these *symmetric* molecules the chains are attached

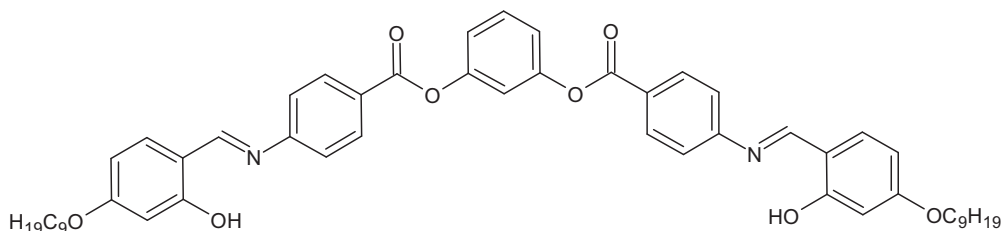


FIG. 2. Structural formula of the compound NORABOW which has been shown to form  $\text{SmC}_g$  layers in Refs. [9,14]. If the hydroxyl groups are absent, only the  $B_2$  phase is formed.

to the core using *ester* linkage groups, and the tilt angles in the intermediate homologs are  $<25^\circ$ . Several *asymmetric* BC molecules form the modulated  $\text{SmC}_{g2}$  phases [17,18]. In one example, the central phenyl ring has a methyl substitution at position 2 of the central phenyl ring, and the phenyl end group of one arm has  $\text{NO}_2$  while that of the other arm has Cl or F substitutions [17]. The compound exhibits a transition from oblique to rectangular 2D lattice as the temperature is lowered. The stripe width in the latter increases rapidly as the temperature is lowered, and the sample undergoes another transition to a nonmodulated bilayer phase. Again, the tilt angle is small,  $\approx 15^\circ$ . Another compound with *symmetric* molecules, with CN groups attached at the ortho position to the alkoxy chains attached to both the terminal phenyl rings exhibits an oblique lattice with bilayer spacing, the tilt angle of the BC molecules being  $\approx 10^\circ$  [17]. A homologous series in which one of the CN groups of the previous compound is replaced by  $\text{NO}_2$  and the other by Cl, with a fixed decyloxy chain at the  $\text{NO}_2$  end, exhibits oblique lattices with bilayers *only while cooling* when the chain lengths at the other end have 10–15 carbon atoms [19]. In all cases the BC molecules which exhibit bilayer structures with or without splay modulation of  $\mathbf{P}$  have the common characteristic of a *relatively low tilt angle*. Another compound with asymmetric BC molecules exhibiting two phases, the higher temperature one being the  $B_7$  and the lower temperature one in which the tilt angle is unusually *reduced*, is suggested to correspond to modulated  $\text{SmC}_g$  phase with *bent* layers [20]. Another interesting case is a compound in which a chemical moiety with a partially silylated chain is connected to one of the arms of a BC molecule through *hydrogen bonding* [21,22]. X-ray scattering studies show that the compound exhibits 2D ordered stripe phases with bilayers. If the chain does not have the silylated group, or if the H bond is replaced by covalent bonding, the stripe phase as well as bilayer structure disappear. We will again

refer to the H-bonded molecules in a later section. To briefly summarize the experimental results, projecting groups like the OH, CN,  $\text{NO}_2$  groups, or silylated chains appear to favor the formation of  $\text{SmC}_g$  and  $\text{SmC}_{gmod}$  phases. Relatively small tilt angles ( $\leq 20^\circ$ , say) are also conducive to the formation of these phases, even in the absence of projecting groups or molecular asymmetry. Interestingly, most of the reported *modulated*  $\text{SmC}_g$  liquid crystals have the *bilayer* structure.

In the following we first point out some geometrical consequences on the packing of molecules in layers when the BC molecules form the  $\text{SmC}_g$  phase. This can be used to rationalize the observation of the  $\text{SmC}_g$  LC in the compounds mentioned above. We also extend our model of the modulated  $B_7$  phase to the compounds exhibiting the stripe phases in some compounds with  $\text{SmC}_g$  layers, pointing out a different feature specific to these materials.

## II. GEOMETRY OF PACKING OF BC MOLECULES IN $\text{SmC}_g$ LAYERS

In the following, we assume that the two arms of the BC molecules have the same length, as several of the compounds found to exhibit  $\text{SmC}_g$  LCs have essentially symmetric molecules (Figs. 2 and 3). In the  $\text{SmCP}$  phases with  $\psi = 0$ , the molecules can pack efficiently in the layers both in a direction parallel to  $\mathbf{P}$ , and in the orthogonal direction. This is no longer true when  $\psi \neq 0$ . The problem is best illustrated for the case  $\psi = \pi/2$  rad, when the tilt and molecular planes are coplanar. Along the direction normal to this plane again a close packing of the molecules is possible [Fig. 4(a)]. However, in the orthogonal direction, if the integrity of the layering is to be maintained, neighboring molecules have to slide along that direction by some distance, which ensures close contact over a reduced length of the lower arms, but the upper arms develop a gap between them [Fig. 4(b)]. This reduces the

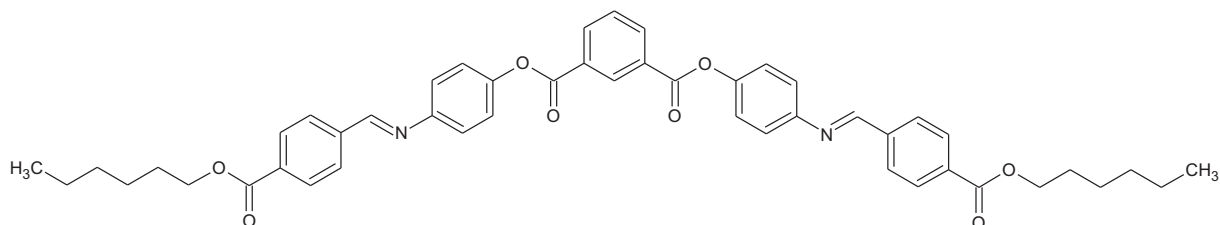


FIG. 3. Structural formula of the compound  $E_{Bm}$  with  $m = 6$ . The homologs with  $m = 10$ –14 exhibit *modulated bilayer* ( $\text{SmCG}_{2mod}$ ) phases [16].

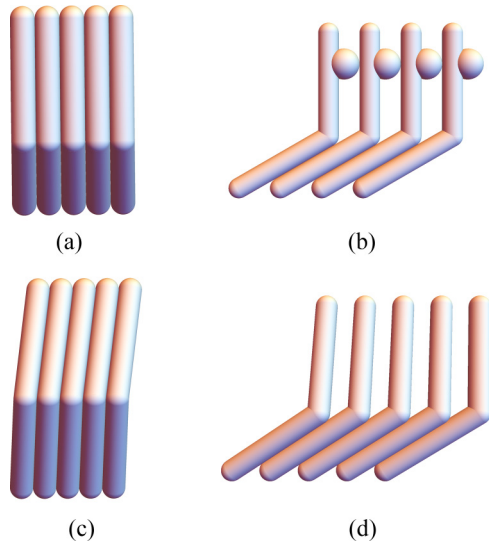


FIG. 4. Geometry of packing of BC molecules in  $\text{SmC}_g$  layers. Top row:  $\psi = 90^\circ$ . (a) The molecules pack well side by side. (b) The molecular packing in the plane containing the arrow axes, such that the layer spacing maintained is less dense. Dipolar groups which protrude from the upper arm (shown symbolically by spherical sections) can favor this packing compared to that in the usual  $\text{SmCP}$  layer with  $\psi = 0$ . Bottom row: When  $0 < \psi < 90^\circ$ , the packing conditions are broadly similar to those at  $\psi = 90^\circ$ .

attractive energy, especially between the upper arms. If  $\psi$  is smaller, as in the general  $\text{SmC}_g$  layer, this geometrical feature persists, though at smaller values of  $\psi$ , the mismatch is also reduced [Fig. 4(d)]. Several compounds which exhibit the  $\text{SmC}_g$  phase have protruding chemical groups on one or both arms, which can then actually favor the formation of  $\text{SmC}_g$  layers, as the groups can fit in the gaps. Further, such groups carry dipole moments, and the lining up of such dipoles in the structure [Fig. 4(b)] is energetically favorable. NORABOW (Fig. 2) has the protruding OH group on both arms, but if say the conformation is such that the group is not in the molecular plane in the lower arm, but the upper arm has the required protrusion in the molecular plane, the  $\text{SmC}_g$  layer structure can be stabilized. BC molecules with such protrusions do not have a more optimal packing in the  $\text{SmCP}$  layers with  $\psi = 0$ . It was noted in [19] that a group protruding at the center of the concave part of the BC molecule can lead to a good packing in the  $\text{SmC}_g$  layers. However, most compounds exhibiting the  $\text{SmC}_g$  phase do not have such centrally located groups.

As mentioned earlier, another strong signature of the  $\text{SmC}_g$  layer structure is the x-ray scattering corresponding to *bilayer* spacing. These are seen in several samples with [17,18,21,22] or without [16,17,19] protrusions from one or both arms, and even when the chemical structure of the molecule is symmetric [16,17]. Except in the compounds with hydrogen bonds [21,22], a common feature of such systems is relatively small tilt angles, with  $\theta \leq 25^\circ$ , and the occurrence of two-dimensional lattices, with one of the spacings in the range of 10s of nanometers. In compounds exhibiting  $\text{SmAP}$  and  $\text{SmCP}$  layers, this structure arises due to formation of stripes in the layers with splay distortion of the polarization [4,5]. As noted earlier, BC molecules which usually have a couple

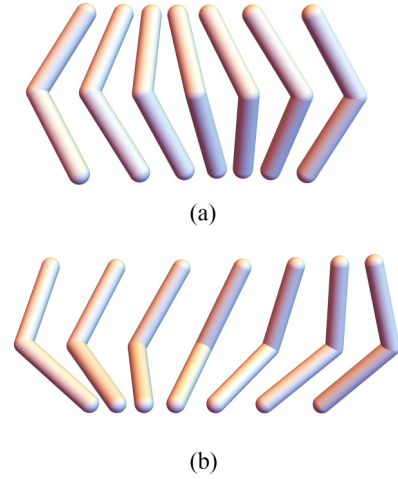


FIG. 5. Schematic figures illustrating the arrangement of the BC molecules in a stripe occurring between nonpolar domains (which are not shown) of (a)  $B_7$  liquid crystal, made of a  $\text{SmCP}$  layer with  $\psi = 0$ , and (b)  $\text{SmC}_g$  LC, with  $\psi \neq 0$ , the splay distortion of  $\mathbf{P}$  resulting from rotation of the BC molecules about the layer normal. The widths of the upper and lower surfaces of the stripe are equal in the  $B_7$  stripe, and unequal in the  $\text{SmC}_g$  stripe.

of ester linkage groups display conformational variety. We have argued earlier [23] that a small fraction ( $\sim 10$ – $20\%$ ) of the molecules has less bent, excited state (ES) conformations. These aggregate to form smecticlike domains in the nematic phase which exhibits many unusual properties of flow, magnetic field enhancement of the nematic-isotropic transition temperature, etc. [23]. In some compounds exhibiting  $\text{SmAP}$  or  $\text{SmCP}$  type layers, the ES conformers can *freely rotate* about their long axes, and the corresponding domains are not polarized. The  $\mathbf{P}$  vector of the ground state molecules with highly bent conformations orients orthogonally to the interface between the two domains, and the positive energy cost is reduced by the allowed splay deformation of the  $\mathbf{P}$  field. We have developed a phenomenological model to account for properties like the temperature variation of the stripe width, the thermodynamically weak first order transition between the modulated and uniform phases, and the effect of an external electric field on the switching and phase transition properties of the medium, etc., of the  $\text{SmAP}_{F_{mod}}$  and  $B_7$  liquid crystals [6,7]. Our aim in this paper is to extend this model to the stripe phase exhibited by the  $\text{SmC}_g$  layers.

### III. MODELS FOR THE STRIPED $\text{SmC}_{g_{mod}}$ PHASE

We consider a single  $\text{SmC}_g$  layer made of BC molecules. Let us recall that in the  $B_7$  stripe phase with  $\text{SmCP}$  layers, the  $\mathbf{P}$  vector which is in the plane of the layer develops a splay distortion by rotating about the layer normal  $\zeta$  from  $-\pi/2$  rad at one wall of the stripe to  $+\pi/2$  rad at the other [Fig. 5(a)]. In a  $\text{SmC}_g$  layer, the  $\mathbf{P}$  vector is not confined to the plane of the layer, but has a component along the layer normal  $\zeta$  as well (Fig. 1). If the layer has the  $\text{SmC}_g$  structure as in NORABOW say, the in-plane component of  $\mathbf{P}$  can be assumed to rotate about  $\zeta$  to form the stripe as in the  $B_7$  phase, and the molecular arrangement in the stripe will have the appearance shown in

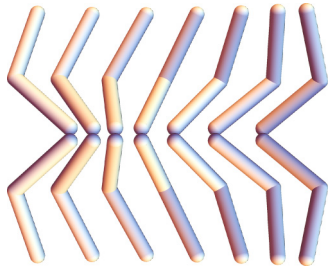


FIG. 6. The  $\text{SmC}_g$  stripe shown in Fig. 5(b) can lower the energy by the formation of bilayers such that the surface widths of adjacent layers match, resulting in an achiral structure in which the net polarization along the layer normal also cancels.

Fig. 5(b). It is clear from the figure that the bent shape of the molecule leads to a *difference* in the length of the upper surface of the striped layer compared to the lower surface. Such stripes cannot obviously be packed uniformly on top of each other as *monolayers*. Thus, the packing of BC molecules in  $\text{SmC}_g$  layers involves geometrical constraints both in uniform and striped structures. The stripes can of course pack as *bilayers* (Fig. 6), as observed in a number of compounds [16–19,21,22]. In the next subsection we will extend our two state model of the  $B_7$  phase to calculate some of the properties of the  $\text{SmC}_g$  stripe schematically shown in Fig. 6. We will also discuss another possible bilayer structure of  $\text{SmCG}_{2\text{mod}}$  phase in which the double tilted molecules rotate about their *long axes* to form the stripes, in Sec. III B.

Vaupotic *et al.* [19] have extended their earlier model of the  $B_7$  phase [24,25], in which the modulation is assumed to arise from the term  $(\nabla \cdot \mathbf{P})|\mathbf{n} \times \boldsymbol{\zeta}|^2$  which couples the molecular tilt and the splay distortion of  $\mathbf{P}$ . The model is extended to the  $\text{SmC}_{g\text{mod}}$  phase by including the term  $|\mathbf{P} \times (\mathbf{n} \times \boldsymbol{\zeta})|$  which describes a general orientation of  $\mathbf{P}$  with respect to the layer [19]. A negative quadratic term combined with a positive quartic term of the coupling can generate a finite general tilt in the smectic layer. However, as discussed in our papers [6,7], the model proposed in [24,25] for the  $B_7$  phase itself has some deficiencies: (i) It cannot lead to the modulated phase in the absence of tilt, though the  $\text{SmAP}_{F\text{mod}}$  phase has been found experimentally [26]. (ii) The calculation made in Ref. [25] was confined to ferroelectric alignment of neighboring stripes across the walls, and the resulting splay angle in the stripe is restricted to  $\sim 20^\circ$  for the stripe width to be in the 10s of nanometer range [25,27] though experiments [26,28] show that it is  $180^\circ$ . (iii) As already noted by the authors of Ref. [5], if successive layers have  $\text{SmC}_aP_F$  structure with anticlinic tilting, in a model of  $B_7$  phase in which the *walls* have a  $\text{div}\mathbf{P}$  distortion reversed with reference to that in the stripe, the elastic energy cost becomes prohibitive. Thus, the model proposed in [25] is unlikely to account for the  $B_7$  stripe phase found in a compound with  $\text{SmC}_aP_F$  layers [29]. In Ref. [17] a compound has been found to exhibit bilayer modulated structure with synclinal tilting of layers at higher temperature, which goes over to an *anticlinic* arrangement in which the layer spacing expands to 100s of nanometers before having a transition to a *monolayer uniform* structure. The authors interpreted the bilayer structures with large stripe widths to be similar to the two-dimensional antiphases which are known to

arise from a competition between monolayer and bilayer spacings in rodlike molecules with highly polar end groups [1,30]. Our model [7] can account for the modulated structures with *anticlinic* layers with *large stripe widths* without invoking any other mechanism. (iv) Further, aging of the samples over some days can increase the stripe width to micrometer range, which becomes visible under a polarizing microscope [5,28], which cannot be explained by the model proposed in Refs. [24,25]. Our alternative model for the modulated phases [6,7] does not have these deficiencies.

As mentioned earlier, the basic assumption in our model is that even the aromatic cores of the BC molecules have considerable flexibility, as they typically have a few ester (COO) linkage groups. The carbon and one of the oxygen atoms of the ester group are connected to successive phenyl rings in the arms of the BC molecule (Figs. 2 and 3) and there is some rotational freedom about these connecting single bonds. The net result is that a fraction ( $\sim 10\text{--}20\%$ ) of the molecules have excited state (ES) *less bent* conformations compared to the ground state (GS) more bent ones. The more bent ones pack with polar order, while the ES conformers can rotate relatively freely about their long axes. They can gain rotational entropy by aggregating in nonpolar domains, and as the local symmetries of the two types of domains are different, they are separated by an interface which costs a positive energy. The polarization ( $\mathbf{P}$ ) of the domain with polar order can be expected to orient along the polar direction which is normal to the interface. This surface order costs a positive polarization energy, which is reduced by the allowed  $\text{div}\mathbf{P}$  distortion of the  $\mathbf{P}$  field. The distorted structure forms stripes between walls of the nonpolar domains made of ES conformers. In the  $B_7$  phase exhibited by a large number of compounds [5], the curvature distortion is brought about by a rotation of the tilted molecules about the layer normal with  $\mathbf{P}$  confined to the plane of the layer, as shown in Fig. 5(a). If the tilt angle is zero, the layer normal coincides with the average orientation direction of the long axes of the GS conformers. Up to now the modulated  $\text{SmAP}_{F\text{mod}}$  phase has been reported only in one compound [26].

In all the compounds which have been found to exhibit the  $\text{SmCG}_{2\text{mod}}$  phase characterized by the bilayer stripe structure, the latter separates directly from the isotropic phase in a first order transition at a temperature  $T_{I\text{mod}}$ , as indeed in most of the samples exhibiting the  $B_7$  phase. We assume that the polar order sets in at a hypothetical second order transition point  $T^*$  which is far above  $T_{I\text{mod}}$ .  $T^*$  corresponds to the transition from the  $\text{SmC}$  phase with relatively freely rotating molecules to the  $\text{SmC}_g$  phase with a polar order of the GS conformers, and the tilt angle  $\theta$  is found to be practically temperature independent even when it is small. For convenience the resulting polarization  $\mathbf{P}$  is taken to be equal to  $p\sigma\mathbf{m}$ ,  $\sigma$  being the *magnitude* of the polar order parameter, given by an appropriate angular average of the molecular dipole moment about the *unit vector*  $\mathbf{m}$  along which  $\mathbf{P}$  is oriented. The proportionality constant  $p$  depends on the dipole moment and the number density of the molecules, assumed to be constant in the temperature range of interest. In order to describe the curvature distortions of the  $\mathbf{m}$  vector in the stripe, we introduce the Cartesian  $\xi\eta\zeta$  coordinate system fixed to the smectic layer (Fig. 7), such that  $\zeta$  is along the layer normal, and  $\xi$  is along the average direction

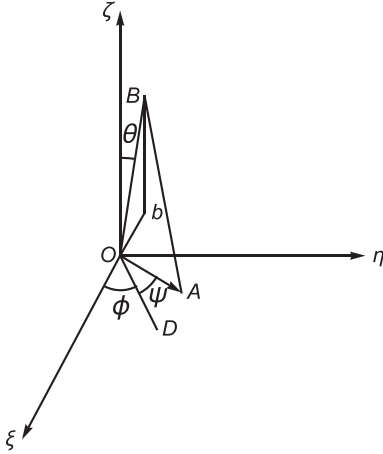


FIG. 7. The orientation of the BC molecule in a stripe caused by the polarization splay in a  $\text{SmC}_g$  layer.  $\zeta$  is along the layer normal of the Cartesian coordinates  $\xi\eta\zeta$  fixed to the layer. The coordinate system  $ABN$  is fixed to the BC molecule, only the upper half of which is shown to avoid clutter. The  $N$  axis, which is orthogonal to the plane  $AOB$  of the molecule is also not shown. The long axis  $OB$  tilts at an angle  $\theta$  from the  $\zeta$  axis.  $OD$  is the line of intersection of the  $\xi\eta$  and  $AN$  planes. If the curvature distortion of  $\mathbf{m}$  occurs by rotation about the layer normal ( $LN$ ), the Eulerian angle  $\psi$  between  $OD$  and  $OA$  is fixed, while the Eulerian angle  $\varphi(\eta)$  varies between the two walls. If the distortion occurs by a rotation about the long axis ( $LA$ ),  $\varphi$  has a fixed value, and  $\psi(\eta)$  varies to form the stripe.

of  $\mathbf{m}$  in the stripe. The molecular coordinate system  $ABN$  is defined such that  $A$  is along the arrow axis,  $B$  is along the long (bow-string) axis, and  $N$  is orthogonal to the molecular plane. The long axis  $OB$  tilts by an angle  $\theta$  from the layer normal  $\zeta$ , and the  $AN$  and  $\xi\eta$  planes intersect along the line  $OD$ . It is clear that  $OA$  makes an angle  $\psi$  with  $OD$ , and  $\varphi$  is the angle made by  $OD$  with the  $\xi$  axis. The orientation of the double tilted BC molecule is described by the Eulerian angles  $\theta$ ,  $\varphi$ , and  $\psi$ .

In the  $\text{SmC}_{gmod}$  phase the free energy density is given by [6,7]

$$\begin{aligned}
 F(\eta) = & \frac{a}{2}(T - T^*)\sigma^2 + \frac{b}{4}\sigma^4 - \alpha(\sigma_S^2 - \sigma^2\mathbf{m}^2)\sigma\nabla \cdot \mathbf{m} \\
 & + \frac{\sigma^2}{2}(\beta_1(\nabla \cdot \mathbf{m})^2 + \beta_2(\mathbf{m} \cdot \nabla \times \mathbf{m})^2 \\
 & + \beta_3(\mathbf{m} \times \nabla \times \mathbf{m})^2) + \frac{p^2\sigma^2}{2\varepsilon\varepsilon_0}m_\eta^2 - p\sigma m_\xi E_\xi, \quad (1)
 \end{aligned}$$

where  $a$  and  $b$  are the usual Landau coefficients, corresponding to the hypothetical transition from nonpolar to polar order mentioned earlier. In liquid crystals made of BC molecules the polarization in smectic layers arises from a polar packing of the molecules, and is not related to molecular tilt. Thus, ferroelectric and more commonly antiferroelectric  $\text{SmAP}$  liquid crystals with upright molecules are found in compounds with BC molecules [4]. Our interest is to account for the occurrence of the *modulated structures* in the layers made of BC molecules, which directly separate from the isotropic phase in a *strong* first order transition. Consequently, both the layering order and the tilt angle are essentially temperature

independent in the liquid crystal. Further, as discussed in our earlier papers [6,7], the *mechanism* for the occurrence of the modulated structures is independent of the molecular tilt in the layers. As such, the Landau coefficients  $a$  and  $b$  describe only the polar order  $\sigma\mathbf{m}$ .  $\alpha\sigma_S^2$  is the coefficient of the term favoring the splay of the  $\mathbf{m}$  field, and  $\alpha$  itself is the coefficient of the  $\sigma^3\mathbf{m}^2\nabla\cdot\mathbf{m}$  term, allowed by the symmetry of the medium with a polar order. As described in our previous papers, this term was originally introduced [31–33] to predict *polarization splay stripes* in ferroelectric LCs made of thin samples of  $\text{SmC}^*$  LCs near  $T^*$ . The  $\alpha\sigma_S^2$  term is a surface term, and cannot generate the splay distortion of  $\mathbf{m}$  in an extended sample. A negative  $\alpha\sigma^3\mathbf{m}^2\nabla\cdot\mathbf{m}$  can generate the stripes as  $\sigma$  itself can also have a spatial variation, coupled to that of spatial variation of  $\mathbf{m}$ . However, the modulated phases ( $B_7$ ,  $\text{SmAP}_{mod}$ , and  $\text{SmC}_{gmod}$ ) exhibited by BC molecules are found in a different regime in most cases, as they are formed when the temperature is lowered from the isotropic phase in a relatively strong *first order* transition. As a result, the order parameter  $\sigma$  does not have a significant spatial dependence unlike in the original model [31–33]. *Both* terms involving  $\alpha$  in Eq. (1) are *surface* terms and the mechanism for the formation of stripes is not that proposed in [31–33]. Moreover,  $\alpha$  is assumed to have a *positive* sign, which is *not favorable* for the formation of stripes. As we have argued in [6,7], the positive sign of  $\alpha$  is likely to be caused by the charge density arising from the splay distortion of  $\mathbf{P}$  [34]. After taking out the mean field dependence on  $\sigma^2$ , the coefficients  $\beta_1$ ,  $\beta_2$ , and  $\beta_3$  are the splay, twist, and bend elastic constants of the  $\mathbf{m}$  field. In both  $B_7$  and  $\text{SmAP}_{mod}$  phases, the  $\mathbf{m}$  field has only bend and splay distortions in the stripe. On the other hand, in the stripe formed in the  $\text{SmC}_{gmod}$  phase (Figs. 5 and 6), both the orientation and location of  $\mathbf{m}$  are not restricted to the central plane of the layer. As a consequence,  $\mathbf{m}$  develops a *twist* distortion *within* the layer across the stripe, the structure being *unique* in that respect. The last but one term of Eq. (1) is the polarization self-energy of the striped sample. Only the  $\eta$  component of the polarization vector is orthogonal to the interface of the stripe with the wall (Figs. 5 and 6), giving rise to this term. It is implicitly assumed that the stripe has an infinite extension along the  $\xi$  and  $\zeta$  axes.

The last term is just  $-\mathbf{P}\cdot\mathbf{E}$  with an electric field  $\mathbf{E}$  acting along the  $\xi$  axis. The components of  $\mathbf{m}$  in the  $\xi\eta\zeta$  system are given by

$$\begin{aligned}
 m_\xi &= \cos\psi \cos\varphi - \sin\psi \cos\theta \sin\varphi, \\
 m_\eta &= \cos\psi \sin\varphi + \sin\psi \cos\theta \cos\varphi, \\
 m_\zeta &= \sin\psi \sin\theta. \quad (2)
 \end{aligned}$$

As we have described above, compounds with a relatively small tilt angle ( $<25^\circ$  say) or those with polar side groups protruding from one or both arms can exhibit the  $\text{SmC}_g$  phase with a general tilt. With this possibility of a *general tilt* in the layer, *two* different types of stripe structures can be imagined.

**A. Stripes in which the curvature distortion of the  $P$  field occurs by rotation of the molecules about the layer normal (LN)**

In our model, we assume that a small fraction of the BC molecules have less bent excited state conformations, and gain

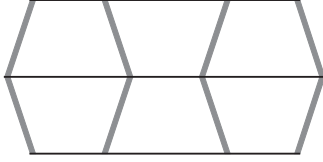


FIG. 8. Schematic diagram showing the disposition of neighboring stripes made of bilayers shown in Fig. 6, forming a two-dimensional rectangular lattice. The shaded areas are made of less bent excited state conformers which rotate freely about their long axes, giving rise to nonpolar walls. The trapeziums symbolically represent the polarization splay stripes made of the more bent ground state conformers (see Figs. 5 and 6).

rotational freedom about their long axes by congregating in the walls of the stripes. From Fig. 5(b), we can see that each monolayer stripe can be approximated as having the shape of a trapezium. Two of them are aligned to form a bilayer stripe (Fig. 6), which can in turn form a two-dimensional structure as shown in Fig. 8. The trapeziums corresponding to neighboring stripes have to be inverted for efficient packing.

They are separated by tilted walls and form a *rectangular* two-dimensional lattice. In the  $B_7$  phase the layer spacing of the walls made of longer ES conformers is somewhat larger than that of the stripes made of GS conformers, and the latter tilt for a better overall packing [5]. However, in the  $\text{SmC}_g$  case as shown in Fig. 8, the walls and polarized stripes have the same layer spacing. Presumably this is possible because the ES conformers of the BC molecules are likely to have considerable flexibility, as the GS conformers can themselves have a double tilt even when the molecular structure is symmetric [9,16]. As in most cases forming stripe phases, the average in-layer component of the polarization  $\mathbf{P}$  of *neighboring stripes* are likely to have *antiferroelectric* alignment especially in sandwich cells to avoid positive electrostatic self-energy, as we have discussed in [6]. The structure of Fig. 6 anyway ensures that the component of  $\mathbf{P}$  along the layer normal averages out.

The angles  $\theta$  and  $\psi$  have fixed values, and as the molecules rotate about  $\zeta$  to form the stripe with a curvature deformation of the  $\mathbf{m}$  field,  $\varphi$  varies along  $\eta$ .

In the field free ( $E = 0$ ) case, with  $\varphi = \varphi(\eta)$  Eq. (1) now reads as

$$F_{LN}(\eta) = \frac{a}{2}(T - T^*)\sigma^2 + \frac{b}{4}\sigma^4 - \alpha(\sigma_S^2 - \sigma^2)\sigma(\cos\psi \cos\varphi - \sin\psi \cos\theta \sin\varphi)\frac{d\varphi}{d\eta} + \frac{\sigma^2}{4}\left(\frac{d\varphi}{d\eta}\right)^2 (A_{0LN} + A_{CLN} \cos 2\varphi + A_{SLN} \sin 2\varphi) + \frac{\sigma^2 p^2}{4\epsilon\epsilon_0}(B_{0LN} + B_{CLN} \cos 2\varphi + B_{SLN} \sin 2\varphi), \quad (3)$$

where

$$\begin{aligned} A_{0LN} &= [1 - (\sin\psi)^2(\sin\theta)^2][\beta_1 + \beta_3 + (\beta_2 - \beta_3)(\sin\psi)^2(\sin\theta)^2], \\ A_{CLN} &= [(\cos\psi)^2 - (\sin\psi)^2(\cos\theta)^2][\beta_1 - \beta_3 - (\beta_2 - \beta_3)(\sin\psi)^2(\sin\theta)^2], \\ A_{SLN} &= \cos\theta \sin 2\psi[\beta_3 - \beta_1 - (\beta_3 - \beta_2)(\sin\psi)^2(\sin\theta)^2], \\ B_{0LN} &= [1 - (\sin\psi)^2(\sin\theta)^2], \\ B_{CLN} &= [(\sin\psi)^2(\cos\theta)^2 - (\cos\psi)^2], \\ \text{and } B_{SLN} &= \sin 2\psi \cos\theta. \end{aligned} \quad (4)$$

The subscript  $LN$  in the above signifies that the structure results from rotation of the BC molecules about the layer normal ( $LN$ ). In the  $B_7$  phase with  $\psi = 0$ , the molecular plane is orthogonal to the tilt plane, and there is no twist distortion in the layer. At the other extreme, with  $\psi = \pi/2$  rad, the two are coplanar and the deformation has a twist component, as indeed for a stripe with any nonzero value of  $\psi$ . The Euler-Lagrange equation, minimizing  $F_{LN}(\eta)$  with respect to  $\varphi$ , involves only the last two terms of Eq. (3). In view of the double tilt of the molecules, the  $\mathbf{m}$  vector will not be along the  $\xi$  axis when  $\varphi = 0$ . Using the fact that at the center of the stripe  $m_\eta = 0$ , the corresponding  $\varphi$  is given by  $\varphi_c = \tan^{-1}(-\tan\psi \cos\theta)$ . For simplicity, we use the one elastic constant approximation, with  $\beta = \beta_1 = \beta_2 = \beta_3$ . The stripe width  $w_{LN}$  is given by

$$w_{LN} = l_{LN} \int_{\varphi_c - \pi/2}^{\varphi_c + \pi/2} \sqrt{\frac{1}{B_{CLN} \cos 2\varphi + B_{SLN} \sin 2\varphi - C_{ILN}}} d\varphi, \quad (5)$$

where  $C_{ILN}$  is the constant of integration, and

$$l_{LN} = \sqrt{\frac{2\epsilon\epsilon_0\beta B_{0LN}}{p^2}} \quad (6)$$

is the length over which the surface polarization is relaxed in the stripe.

The free energy density, *averaged* over the stripe width  $w_{LN}$ , can be written as

$$\begin{aligned} \bar{F}_{LN} &= \frac{a}{2}(T - T^*)\sigma^2 + \frac{b}{4}\sigma^4 + \frac{2\gamma\sigma^2}{w_{LN}} \\ &\quad - \frac{2\alpha(\sigma_S^2 - \sigma^2)\sigma}{w_{LN}}(\cos\psi \cos\varphi_c - \sin\psi \cos\theta \sin\varphi_c) \\ &\quad + \frac{\sigma^2 p^2}{4\epsilon\epsilon_0}(B_{0LN} - C_{ILN}) + \frac{\sigma^2 p^2}{2\epsilon\epsilon_0 w_{LN}} \int_{-w_{LN}/2}^{w_{LN}/2} \\ &\quad \times (B_{CLN} \cos 2\varphi + B_{SLN} \sin 2\varphi) d\eta, \end{aligned} \quad (7)$$

where we have included the interfacial energy  $2\gamma\sigma^2$  from the interfaces at the two walls of the stripe, taking into account its mean field (quadratic) dependence on the order parameter and the symbol  $LN$  signifies rotation of the molecules around the layer normal.

The polarization of the stripe phase is given by the spatial average

$$P_{\text{str}} = \frac{p\sigma}{w_{LN}} \int_{-w_{LN}/2}^{w_{LN}/2} m_{\xi} d\eta. \quad (8)$$

We can note however that many compounds which exhibit the  $\text{SmCG}_{2\text{mod}}$  phase have symmetric molecules without any protruding side groups (Fig. 3). As we discussed earlier, the packing of these molecules in the striped layers (Fig. 4) is subject to some geometrical constraints. In the series with the structural formula shown in Fig. 3, in which switching of the polarization by an electric field above a threshold value has been studied, it was found that the process takes place by *rotation* of the molecules about their *long axes* [16]. Only above a second threshold, the faster variation of the imposed electrical torque leads to the switching by a rotation of the molecules about the layer normal [16]. Indeed a similar change in the switching mechanism has been found in the  $\text{SmCP}$  phases of many other compounds with BC molecules [35,36]. Electric field induced switching by rotation around the long axes was found in the  $B_{1\text{RevTilted}}$  phase of a compound [37] if the applied field was triangular in shape, while it changed over to switching by rotation about layer normal for a square wave field. A theoretical analysis based on the model of Refs. [24,25] showed that the former process is possible *only* in cases with a small stripe width ( $\sim 5$  nm), and if the stripe width is large ( $\sim 50$  nm), the switching occurs by rotation of the molecules about the layer normal [37]. The switching of  $\mathbf{P}$  under the action of  $\mathbf{E}$  is a dynamic process, whose analysis requires appropriate rotational viscosities to be taken into account [35–37].

In the following section, we assume that the formation of the equilibrium stripe structures can result from rotation of the BC molecules around their long axes, rather than about the layer normal considered above. Further, the latter process generates only rectangular 2D lattices (Fig. 8), while in most cases the  $\text{SmCG}_{2\text{mod}}$  phase exhibits oblique lattices [17–19,21,22]. It was mentioned in Ref. [19] that the splay deformation could occur by rotation of BC molecules around their long axes, though in the analysis its effect is mainly seen only in the wall region with *unfavorable* splay distortion of the polarization, in which the tilt angle itself tends to 0 [19,24,25]. In the proposed structure of the bilayer stripe shown in Fig. 1(d) of Ref. [19] the geometric molecular center has a constant height across the stripe, which hence corresponds to rotation of the molecules about the layer normal, as in Fig. 5(b). In the following, we extend our theoretical model to the process of molecular rotation about the long axes, before we present calculations based on both processes.

### B. Model of stripe formation by rotation of the BC molecules about their long axes (LA)

This case corresponds to the long axis of the BC molecule fixed along a well defined orientation in the layer, the defor-

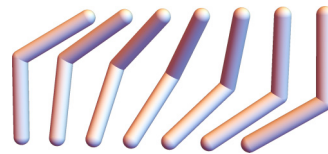


FIG. 9. Schematic diagram showing the disposition of molecules in a polarization splay stripe formed by the rotation of the molecules about their *long axes* which are confined to the  $\eta\zeta$  plane, corresponding to  $\varphi = 0$  in Fig. 7. The rotation angle  $\psi = 0$  at the center of the stripe, and varies from  $-\pi/2$  rad at the left edge to  $+\pi/2$  rad at the right edge, exploring all values in between. The location along  $\zeta$  of the arrow axis ( $A$  in Figs. 1 and 7) also varies across the stripe. The upper and lower surfaces of the stripe have *equal* widths unlike in the structure shown in Fig. 5(b), but relatively displaced along the  $\eta$  axis.

mation of the  $\mathbf{m}$  field arising from rotation of the arrow axis about the long axis. Referring to Fig. 7, the angles  $\theta$  and  $\varphi$  are fixed, while  $\psi$  varies along  $\eta$ . Two extreme cases are of interest. When  $\varphi = 0$  rad, the tilt plane (and hence the long axis) is confined to the  $\eta\zeta$  plane. The schematic diagram of a stripe formed by molecular rotation about the long axes in this case is shown in Fig. 9.

First, the structure explores all values of  $\psi$ , from 0 to  $\pm\pi/2$  rad. We note that unlike in the case of stripe formation by rotation of the BC molecules about the layer normal [Fig. 5(b)], in the present case, the upper and lower surfaces of the stripe have the same width, though there is a relative shift of the two (Fig. 9). The structure can be represented by a parallelepiped, instead of a rectangle as in the case of  $B_7$  phase [Fig. 5(a)]. The stripes can in principle stack up one on top of the other to form a necessarily oblique lattice made of monolayers. However, it is clear that formation of bilayers as shown in Fig. 10 is more favorable, as it results in a stronger *interlayer* van der Waals interaction at one end and facile interlayer fluctuations of the molecules at the other end of the stripe.

The orientations of  $\mathbf{m}$  in the two layers have to be preferentially parallel at the center of the stripe to exploit the above interactions, i.e., in a given stripe the layers have a

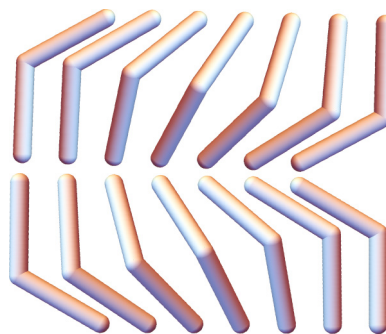


FIG. 10. The mutual interaction energy between successive  $LA$  type stripes can be lowered if they form bilayers as shown in the figure, with the BC molecules at the left end gaining entropically by easy fluctuation between the two layers, and those at the right end by van der Waals interactions, and a combination of the two in between. Both the net chirality and the component of the polarization along the layer normal  $\zeta$  of the bilayer structure are 0.

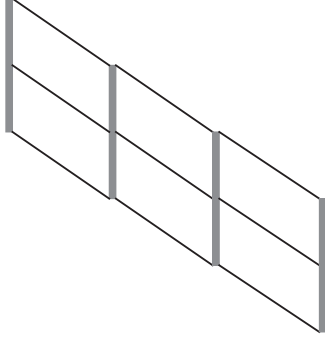


FIG. 11. Schematic diagram of a two-dimensional oblique lattice formed by the bilayers shown in Fig. 10. The vertical shaded regions are nonpolar walls made of freely rotating ES conformers. The parallelepipeds in between the walls represent the stripes made of GS conformers. If neighboring stripes tilt in opposite directions, a rectangular lattice results [5,7].

ferroelectric order. The chiralities of the two layers have opposite sense, and further, the net component of the polarization along the layer normal of the bilayer is zero. As usual, neighboring *stripes* will probably have an antiferroelectric orientation. The shape of the bilayer is closer to a rectangle compared to that of either layer, and the stripes can form either oblique or rectangular 2D lattice as in the case of the usual  $B_7$  phase [38] (Fig. 11).

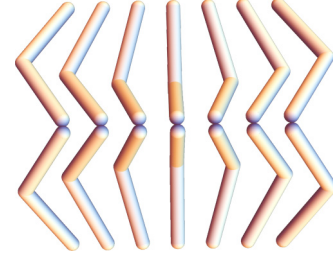


FIG. 12. Schematic diagram showing a bilayer made of adjacent layers in which polarization splay stripes have formed by rotation of the BC molecules about their long axes, which are confined to planes parallel to the  $\zeta\xi$  plane, corresponding to  $\varphi = \pi/2$  rad in Fig. 7. The angle  $\psi = \pi/2$  rad at the center, and varies from 0 to  $\pi$  rad between the two edges of the stripe.

The other extreme case occurs when  $\varphi = 90^\circ$ , with the tilt plane containing the long molecular axis being parallel to the  $\zeta\xi$  plane (see Fig. 7). A bilayer structure formed by stripes with this characteristic is shown in Fig. 12. Notably, unlike in the structures shown in Figs. 5(b) and 9, the  $\mathbf{m}$  vector is orthogonal to the interfaces with the nonpolar domains at both ends of the stripe, and further, each layer has an essentially rectangular shape. Both these features are similar to those of the stripes formed in the  $B_7$  phase [Fig. 5(a)].

The  $\xi$ ,  $\eta$ , and  $\zeta$  components of  $\mathbf{m}$  are again given by Eq. (2). In the general case with  $\psi = \psi(\eta)$  the free energy density of the stripe is now given by

$$\begin{aligned}
 F_{LA}(\eta) = & \frac{a}{2}(T - T^*)\sigma^2 + \frac{b}{4}\sigma^4 - \alpha(\sigma_S^2 - \sigma^2)\sigma(\cos\theta \cos\varphi \cos\psi - \sin\varphi \sin\psi) \frac{d\psi}{d\eta} \\
 & + \frac{\sigma^2}{4} \left( \frac{d\psi}{d\eta} \right)^2 (A_{OLA} + A_{CLA} \cos 2\psi + A_{SLA} \sin 2\psi) + \frac{\sigma^2 p^2}{4\epsilon\epsilon_0} (B_{OLA} + B_{CLA} \cos 2\psi + B_{SLA} \sin 2\psi) \\
 & - E_\xi p \sigma (\cos\varphi \cos\psi - \cos\theta \sin\varphi \sin\psi),
 \end{aligned} \tag{9}$$

where

$$\begin{aligned}
 A_{OLA} &= (\beta_1 + \beta_3) + (2\beta_2 - \beta_1 - \beta_3)(\sin\theta)^2(\cos\varphi)^2, \\
 A_{CLA} &= (\beta_1 - \beta_3)[(\cos\theta)^2(\cos\varphi)^2 - (\sin\varphi)^2], \\
 A_{SLA} &= (\beta_3 - \beta_1)\cos\theta \sin 2\varphi \\
 B_{OLA} &= 1 - (\sin\theta)^2(\cos\varphi)^2 \\
 B_{CLA} &= [(\sin\varphi)^2 - (\cos\theta)^2(\cos\varphi)^2], \\
 \text{and } B_{SLA} &= \cos\theta \sin 2\varphi.
 \end{aligned} \tag{10}$$

In the above, the subscript  $LA$  signifies a structure generated by rotation of the BC molecules about their long axes, and  $E_\xi$  is a DC electric field acting along  $\xi$ . Only the stripe structure with  $\varphi = \pi/2$  rad shown in Fig. 12 is free from twist distortion in the layers. Again, for a given value of  $\varphi$ ,  $m_\eta = 0$  at the center of the stripe which corresponds to the value of  $\psi = \psi_c = \tan^{-1}(-\tan\varphi/\cos\theta)$ . As before, using the one elastic constant ( $=\beta$ ) approximation, the minimization of the free energy given by Eq. (9) with respect to  $\psi(\eta)$  results in the following stripe width  $w_{LA}$ :

$$w_{LA} = l_{LA} \int_{\psi_c - \pi/2}^{\psi_c + \pi/2} \frac{d\psi}{\sqrt{B_{CLA} \cos 2\psi + B_{SLA} \sin 2\psi - r_{ELA}(\cos\varphi \cos\psi - \cos\theta \sin\varphi \sin\psi) - C_{ILA}}}, \tag{11}$$

where the length  $l_{LA} = \sqrt{2\varepsilon\varepsilon_0\beta}/p$ ,  $r_{ELA} = 4E_\xi\varepsilon\varepsilon_0/(\sigma p)$ , and  $C_{ILA}$  is a constant of integration. The free energy density averaged over the stripe width is given by

$$\begin{aligned} \bar{F}_{LA} = & \frac{a}{2}(T - T^*)\sigma^2 + \frac{b}{4}\sigma^4 + \frac{2\gamma\sigma^2}{w_{LA}} - \frac{2\alpha(\sigma_S^2 - \sigma^2)\sigma}{w_{LA}}(\cos\theta\cos\varphi\cos\psi_c - \sin\varphi\sin\psi_c) + \frac{p^2\sigma^2}{4\varepsilon\varepsilon_0}(B_{0LA} - C_{ILA}) \\ & + \frac{\sigma^2 p^2}{2\varepsilon\varepsilon_0 w_{LA}} \int_{-w_{LA}/2}^{w_{LA}/2} [B_{CLA} \cos 2\psi + B_{SLA} \sin 2\psi - r_{ELA}(\cos\varphi\cos\psi - \cos\theta\sin\varphi\sin\psi)] d\eta. \end{aligned} \quad (12)$$

#### IV. RESULTS AND DISCUSSION

We first consider the structures in the absence of an external electric field, so that  $E_\xi = r_{ELA} = 0$  in Eqs. (9), (11), and (12). The  $LN$  structure goes over to that of the usual  $B_7$  case if  $\psi = 0$  (Figs. 1 and 7), and as  $\varphi_c = 0$  in this case,  $l_{LN}$  [from Eq. (6)] becomes equal to  $l_{LA}$  defined after Eq. (11). In addition, if the angle  $\varphi = \pi/2$  rad in the  $LA$  case, corresponding to the structure shown in Fig. 12,  $\psi_c = -\pi/2$  rad and the expressions for the stripe width [Eq. (5)], and the free energy density averaged over the stripe width [Eqs. (7) and (12)] in the field free case become identical in the  $LN$  and  $LA$  cases, and the tilt angle  $\theta$  drops out of the problem in both cases. Further, if  $\theta = 0$  corresponding to the  $SmA$  phase, the expressions for the stripe width [Eqs. (5) and (11)] and the averaged free energy density given by Eqs. (7) and (12) are again identical, as they should be, since there is no physical difference between the two processes in this case, and in these cases, there is *no twist* distortion in the stripe.

For comparing the two cases in more general cases, we use the following values for the parameters of the model, as in our earlier papers [6,7]:  $\alpha = 10^4 \text{ J K m}^3$ ,  $b = 14 \times 10^5 \text{ J m}^{-3}$ ,  $\alpha = 5.5 \times 10^{-4} \text{ J m}^{-2}$ ,  $\beta = 2.5 \times 10^{-12} \text{ J m}^{-1}$ ,  $\gamma = 2 \times 10^{-5} \text{ J m}^{-2}$ ,  $p = 3.5 \times 10^{-3} \text{ C m}^{-2}$ , and  $\varepsilon\varepsilon_0 = 40 \times 10^{-11}$ . Again with  $E_\xi = 0$  initially, the calculations are done as follows: For a given pair of the Eulerian angles  $\theta$  and  $\psi$  (in the  $LN$  case) or  $\varphi$  (in the  $LA$  case), and at any given relative temperature  $T^* - T$ , the stripe width  $w$  is determined by the appropriate integration constant  $C_I$ . The averaged free energy density given by Eqs. (7) or (12) is then minimized with respect to the order parameter  $\sigma$ . Using an iterative scheme,  $w$  and  $\sigma$  are adjusted to get the absolute minimum of the free energy density. The free energy density of the *uniform* phase without the stripes is given by just the first two terms of Eqs. (7) or (12). The phase with a lower value of  $\bar{F}$  is the stable phase at the given relative temperature. The main results are as follows: As in the case of the  $B_7$  phase [7], the stripe

phase is more stable at higher temperatures. The stripe width increases as the temperature is lowered. At some relative temperature  $T^* - T_{tr}$ , there is a *weak* first order transition to the uniform phase with a *small* jump in the order parameter  $\sigma$ . We summarize the dependencies of the relative transition temperature ( $T^* - T_{tr}$ ) and the stripe width at the transition point ( $w_{tr}$ ) on the appropriate angles in Table I for the  $LN$  case and Table II for the  $LA$  case. As discussed in the previous paragraph, the transition properties are independent of the tilt angle  $\theta$  when  $\psi = 0$  in the  $LN$  process, and  $\varphi = \pi/2$  rad in the  $LA$  process. The data bring out the dependencies *purely* on the *relevant angles*, without taking into account the dependencies of the parameters of the phenomenological theory on those angles. The variations become stronger as the tilt angle increases, with the transition temperature  $T_{tr}$  being quite sensitive to  $\psi$  in the  $LN$  case, whereas the stripe width  $w_{tr}$  at  $T_{tr}$  has a strong dependence on  $\varphi$  in the  $LA$  case. Properties like the elastic constant  $\beta$  can be expected to vary substantially with the tilt angle  $\theta$ . Further, in the  $LN$  case the deformation of the  $\mathbf{m}$  field inevitably leads to that of the  $\mathbf{c}$ -vector field, increasing the effective elastic constant. As no experimental data are available on the relevant parameters, we do not present dependencies of the transition properties on these parameters of the problem. In general a higher value of the elastic constant  $\beta$  increases the stripe width  $w$ . For example, in the  $LA$  case, with  $\theta = 45^\circ$  and  $\varphi = 90^\circ$ , if  $\beta$  is decreased to  $1.2 \times 10^{-12} \text{ J m}^{-1}$ , the stripe width decreases to 32.98 nm, and  $T^* - T_{tr}$  increases to 98.19 K, compared to the data of Table II. The main effect of a change in the value of  $\alpha$  is on the transition temperature. For example, if  $\alpha$  is reduced from  $5.5 \times 10^{-4} \text{ J m}^{-2}$  to  $2 \times 10^{-4} \text{ J m}^{-2}$ , the relative transition temperature changes from 98.19 to 51.635 K in the  $LA$  case considered above.

We have made some calculations on the effect of a DC electric field  $E_\xi$  acting along the  $\xi$  axis on the  $LA$  structure with  $\varphi = 90^\circ$  shown in Fig. 12. We may recall that in the absence of the field, the stripe width at any  $T$ , including  $T_{tr}$ ,

TABLE I. Transition properties for the  $LN$  process.

	$\psi = 0^\circ$	$\psi = 45^\circ$	$\psi = 90^\circ$
Relative transition temperature $T^* - T_{tr}$			
$\theta = 10^\circ$	83.84 K	84.12 K	84.38 K
$\theta = 45^\circ$	83.84 K	88.65 K	94.58 K
Stripe width $w_{LN}$ at $T_{tr}$			
$\theta = 10^\circ$	55.57 nm	55.54 nm	55.49 nm
$\theta = 45^\circ$	55.57 nm	56.49 nm	57.55 nm

TABLE II. Transition properties for the  $LA$  process.

	$\varphi = 0^\circ$	$\varphi = 45^\circ$	$\varphi = 90^\circ$
Relative transition temperature $T^* - T_{tr}$			
$\theta = 10^\circ$	83.74 K	83.79 K	83.84 K
$\theta = 45^\circ$	81.72 K	82.92 K	83.84 K
Stripe width $w_{LA}$ at $T_{tr}$			
$\theta = 10^\circ$	56.94 nm	56.28 nm	55.57 nm
$\theta = 45^\circ$	91.17 nm	68.50 nm	55.57 nm

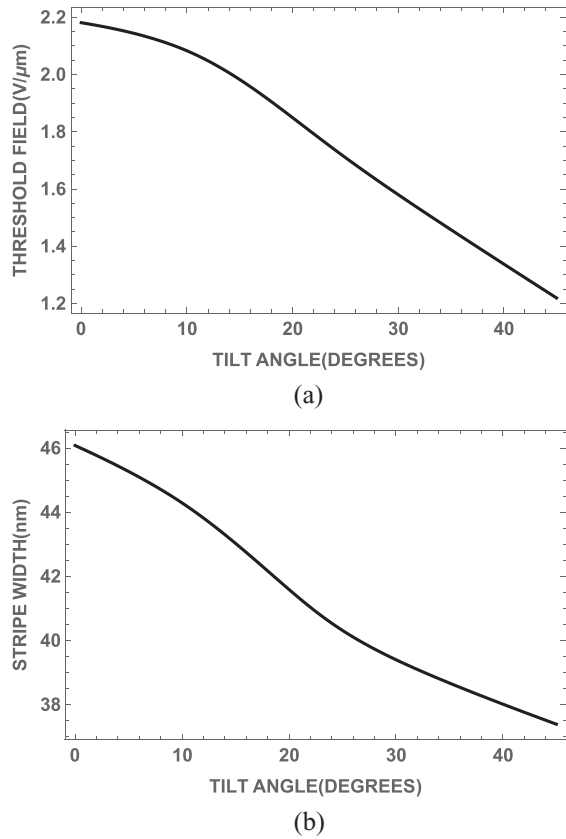


FIG. 13. Tilt angle dependencies of (a) the threshold field  $E_{th}$  and (b) the stripe width at threshold as functions of the tilt angle  $\theta$  at  $T^* - T_{tr} = 75$  K, with the parameters given in the first paragraph of this section, for the stripe having  $LA$  structure with  $\varphi = 90^\circ$ . In the absence of the field, the stripe width is 35.08 nm independent of  $\theta$ .

is independent of the tilt angle. Assuming that all the stripes are oriented with the average  $\xi$  component of the polarization  $P_\xi$  having a positive sign, the stripe width increases with  $E$ , and at some threshold value  $E_{th}$ , there is a transition to the uniform phase, as in the case of the usual  $B_7$  phase [5–7]. The uniform phase is assumed to be the usual  $B_2$  with the polarization vector confined to the layer plane, corresponding to that adjacent to the wall (Fig. 12). The electric field enhances the order parameter  $\sigma$  and as the tilt angle  $\theta$  is increased, the lowered free energy density due to the field of the uniform phase catches up with that of the stripe phase at a lower value of  $E$ , as can be expected from the structure shown in Fig. 12. As mentioned earlier, in the field free case when  $\varphi = 90^\circ$ , the tilt angle drops out from Eqs. (10)–(12). However, this is no longer true when an electric field acts on the sample [see Eq. (12)]. The threshold field  $E_{th}$  as well as the stripe width at the threshold decrease with the tilt angle  $\theta$  at a fixed relative temperature. The results at  $T^* - T_{tr} = 75$  K are shown in Fig. 13. We emphasize that we have studied only the effect of changes in the tilt angle  $\theta$ , without taking into account the changes in the other parameters like  $\beta$  with  $\theta$ . Further, the orthogonal anchoring of  $\mathbf{P}$  at the interface is assumed to be infinitely strong, while in reality, it is more likely to have a finite value.

In the following, we recall some interesting aspects of the experimental results on two very different types of chemical species in which some detailed studies have been made. The first species consists of symmetric molecules, whose basic structure is shown in Fig. 3. We indicate the homologs by the symbol  $E_{Bm}$ , where  $m$  is the number of carbon atoms in the end chains. The bilayer structures are exhibited only for  $m = 10$ –14 [16]. Only uniform  $SmCP_A$  phases with monolayers are exhibited by the homologs with  $m = 7$ –9. Interestingly, beyond a threshold field, the compounds exhibit polarization switching around electric field  $E = 0$  described as a nonclassical ferroelectric [16] or superparaelectric [39] phase by the authors. This shows that these homologs with small  $m$  values have a high polarization  $\mathbf{P}$ , and consequently in the field induced ferroelectric phase,  $\mathbf{P}$  orients perpendicular to the electrodes as discussed in [40]. The high value of  $\mathbf{P}$  also prevents the formation of stripes, as the positive energy of the last but one term in Eq. (1) dominates. As the chain length is increased to  $m = 10$ , the medium exhibits a higher temperature bilayer to a lower temperature monolayer phase transition, and again exhibits the superparaelectric characteristics beyond some  $E_{th}$  at low temperatures. However, at higher temperatures when  $\mathbf{P}$  has relatively low values, the medium probably has bilayer structure, switching by rotation about long axes just above a first  $E_{th}$ , and beyond a higher threshold at which the field fully reorients the  $\mathbf{P}$  vectors of all the layers, the “super paraelectric” response is seen [39]. It is quite likely that  $\mathbf{P}$  has reduced sufficiently for the formation of stripes when  $m = 10$ , especially as the tilt angle is sufficiently low ( $\sim 25^\circ$ ). The stripe width  $w$  may be large enough to be inaccessible for detection by x rays, if the elastic constants also have sufficiently high values. It is also very likely that the stripes are formed by rotation of the BC molecules around their long axes ( $LA$ ), as indicated by the switching characteristics. The lower temperature phase is the uniform monolayer phase, and it is quite likely that the formation of *bilayers* at higher temperatures is a natural consequence of the  $LA$  structure of the *stripe* phase. As  $m$  is increased further, the tilt angle is reduced, the polarization can also be in the sweet range for the formation of stripes, though the samples crystallize before forming lower temperature uniform phase [16]. The elastic constants, and hence the stripe width  $w$  also decrease as  $m$  is increased. When  $m$  is increased to 15 and 16,  $\theta \approx 10^\circ$  is sufficiently small, and  $E_{th}$  for the switching by rotation about the long axis itself decreases with  $m$  (and temperature). At higher fields, instead of going over to the superparaelectric type of behavior above a second threshold field, the switching occurs by rotation of the BC molecules around the layer normal, as found in some other BC compounds [35–37]. It is reported that the  $m = 15$  and 16 homologs exhibit at higher temperatures a monolayer stripe phase (with low  $w \approx 15$  nm) which transforms to the uniform phase as the temperature is lowered [16]. The authors note that the diffuse wide angle x-ray scattering shows *two* humps corresponding to  $\theta \approx 10^\circ$ , while the layer spacing  $d$  essentially corresponds to the molecular length  $l$ . It is quite possible that the stripe phase may be made of bilayers as in the lower homologs, but the low value of  $\theta$  may make the x-ray spot corresponding to the bilayer spacing of the symmetric molecules too weak for detection.

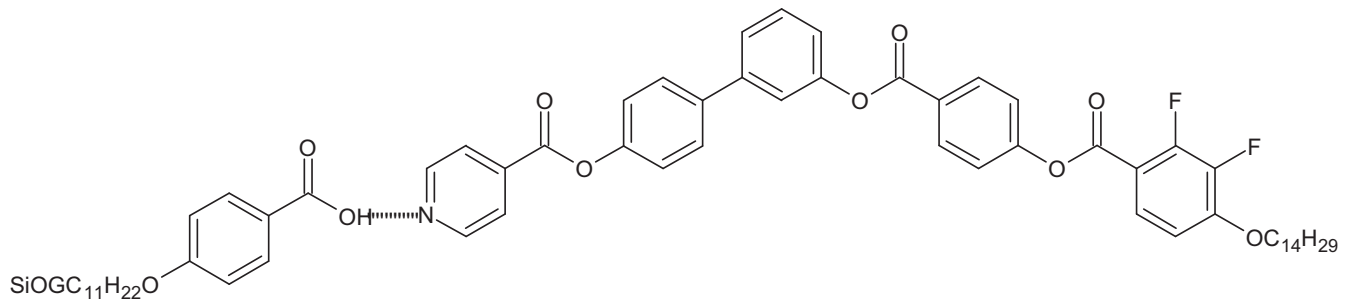


FIG. 14. General structural formula of an asymmetric bent-core molecule with the left side arm connected by a hydrogen bond to a chemical group which has a few different moieties made of siloxanes and indicated by the symbol SiOG at the end of undecyloxy chain. The line between the hydroxyl (OH) group and the nitrogen (N) atom stands for the hydrogen bond between them. Compounds with this structure exhibit bilayer stripe phases when SiOG is a short linear moiety oriented either along or orthogonal to the axis of the arm, or even a relatively bulky group [21,22]. Both the SiOG group and the H bond are necessary for the formation of stripes, which are not exhibited in the absence of either of them.

Another interesting variety of BC compounds exhibiting the  $\text{SmCG}_{2\text{mod}}$  phase has a *hydrogen bond linking* one of the arms of a bent core, with a chemical moiety with a relatively large structure made of siloxane groups located at the end of an alkoxy chain. The other arm of the BC molecule has only a long alkoxy chain (Fig. 14) [21,22]. Interestingly, the  $\text{SmCG}_{2\text{mod}}$  phase has been found with different types of large groups made of SiO units, but if the *large groups are removed*, the modulated phase is *not observed*. Further, if the H bond is replaced by a *covalent bond*, the *modulations disappear* in all the cases, even with the large groups. We can understand this observation on the basis of the model presented above as follows. The strength of the H bond is relatively weak, and weakened further at higher temperatures as indicated by spectroscopic measurements [21,22]. As such, we can expect that in a small fraction of the BC molecules, the bonds can break, so that the resulting moieties which are *shorter* than the unbroken molecules act as *impurities*. They can then aggregate to form the walls which can be thought of as having a layering with a *smaller* spacing compared to the unbroken tilted BC molecules. We can then expect the processes discussed earlier to lead to the formation of the stripe structure, with one main difference. As the effective layer spacing of the wall is *smaller* than that of the stripe made of unbroken molecules, the *walls tilt* for an efficient packing (Fig. 15), unlike in the usual modulated structures where the stripes tilt (Fig. 11). It is clear that in compounds in which the H bonds are replaced by covalent bonds, the above process and hence the stripe phase is absent.

The structure can exhibit either oblique or rectangular lattice, depending on the relative location of the second neighbor stripe along the  $\eta$  axis. Indeed in one of the compounds, both types of lattices have been found [22]. Another unusual feature of the bilayer stripe phase of the H-bonded BC compounds is the large tilt angle  $\theta$ ,  $> 50^\circ$ . (We may note that  $\theta$  is equivalent to the “leaning angle” as defined by the authors in Fig. 1 of Ref. [22].) This has been measured by the location of the humps in the wide angle scattering corresponding to the width of the molecules in oriented samples obtained by a DC electric field. The structures of the bilayer stripes shown in Figs. 10 and 12 naturally give rise to these humps in the scattering. If the size of the end siloxane group is not very

large, the H-bonded compounds exhibit a higher temperature oblique lattice going over to either a rectangular or an undulated 2D lattice at lower temperatures [21,22]. On the other hand a very large end group gives rise to only the oblique lattice. Electro-optic studies have been used to conclude that at higher temperatures, the switching occurs by *rotation around the long axes*, supporting the LA structure (Figs. 10 and 12). In the uniform phase obtained at low temperatures, the switching is by rotation about the layer normal [21,22]. As the chemical structures of the BC molecules shown in Figs. 3 and 14 are rather different, it is not possible to compare the results on, say, the threshold field  $E_{\text{th}}$  with our theoretical calculations, in which only the tilt angle  $\theta$  has been varied, keeping all other parameters unaltered. This is unlikely to be true even for different homologs of the series shown in Fig. 3. The interesting common observation in all the experimental systems is that the switching occurs by a rotation about the long axes above a first threshold.

## V. CONCLUSIONS

The triclinic  $\text{SmC}_g$  phase with a stacking of *fluid* layers made of molecules with shape anisotropy is quite exotic. The polar packing of the BC molecules in layers

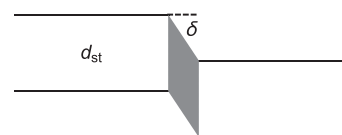


FIG. 15. Schematic diagram showing a possible origin of the stripe phases exhibited by the H-bonded BC molecules shown in Fig. 14. The fragments of the molecules in which the hydrogen bonds are broken are assumed to collect in the wall region shown by the shaded part, and form nonpolar layers. The unbroken molecules form the stripes made of bilayers (see Fig. 12) with a spacing equal to  $d_{\text{st}}$  and large ( $> 50^\circ$ ) tilt angles. The layer spacing of the wall region ( $d_{\text{wall}}$ ) can be expected to be smaller than  $d_{\text{st}}$  unlike in the usual BC molecules, and the wall itself has to tilt at an angle  $\delta = \cos^{-1}(d_{\text{wall}}/d_{\text{st}})$ , to fill space. The stripes can form either an oblique or a rectangular 2D lattice, depending on the relative location of the second neighbor stripe.

facilitates such a molecular arrangement. However, the geometrical constraints in the packing of the BC molecules in the  $\text{SmC}_g$  layer restrict its occurrence to a small number of cases. Chemical groups projecting preferably from one of the arms of the BC molecules can lead to a better packing in the  $\text{SmC}_g$  layer compared to that in the  $\text{SmCP}$  layer of the  $B_2$  phase in which the average molecular dipole moment is in the plane of the layer. The geometrical constraint is diminished if the tilt angle is relatively small. Optical measurements on defect structures in free standing films have been used to directly measure the two angles needed to describe the molecular orientation in the layers. In both systems used in such measurements, uniform  $\text{SmC}_g$  layers have been found. Another clear signature of the general tilting is in the occurrence of bilayers in several compounds made of BC molecules. In most of them, the bilayers form *stripes*. We have extended our model of the striped  $B_7$  phase to this case. The experimental results are better accounted for if the splay distortion of the polarization in the layers occurs by a rotation of the BC molecules about the long axes, rather than about the layer normal. In the former case, the  $\mathbf{c}$ -vector field does not have any curvature distortion, and the elastic constant of the splay deformation of  $\mathbf{P}$  is reduced. In our model, the conformational variety of BC molecules is the main cause for the spatial nonuniformities of the structures exhibited in both the nematic [23] and striped-smectic [6,7] phases. Less bent molecules (i.e., excited state conformers) have rotational freedom about their long axes, which form nonpolar domains in the smectic layers, and the polarized domains made of more bent ground state conformers form the stripes with polarization splay between the nonpolar domains, if  $\mathbf{P}$  is not too high. In the samples exhibiting the  $\text{SmC}_g$  structure, the stripes preferentially form by a rotation of the BC molecules about their long axes, and the resulting domain necessarily results in a bilayer structure (Figs. 10 and 12). In fact, even in BC molecules with H bonds, even though the tilt angle is

relatively large, it appears that the H bonds break in a small fraction of the molecules, which can in turn form the nonpolar domains, with an effective layer spacing smaller than that of the polarized domains. The polarization splay stripes again form by a rotation of the molecules about their long axes, resulting in a bilayer structure.

In conclusion, the conformational variety or the possibility of molecular dissociation is the main cause for the occurrence of the stripe structures exhibited by BC molecules with  $\text{SmC}_g$  layers. Further, it is very likely that the polarization  $\mathbf{P}$  is strongly anchored orthogonally to the interface between the polar and nonpolar domains, as shown in Figs. 5(a) and 12, rather than at an angle as required in the structures shown in Figs. 5(b) and 10. If the curvature distortion occurs by a rotation of the BC molecules about the layer normal, the  $B_7$  type stripe shown in Fig. 5(a) results, as in a large number of compounds [5,7]. On the other hand, if the distortion occurs by a rotation of the molecules about their long axes, the  $\text{SmC}_{gmod}$  phase with a *bilayer* structure results, as in Fig. 12, and is exhibited by a relatively small number of compounds. A previously proposed model requires a new coupling to account for the  $\text{SmC}_{gmod}$  phase [19], and attributes the large stripe widths measured in some  $\text{SmC}_{gmod}$  liquid crystals to arise from a competition between monolayer and bilayer structures [17]. However, as we noted earlier, even the  $B_7$  phase can exhibit large values of  $w$ , even though there is obviously no competition between two layer spacings in this case.

Our model of the modulated phases gives a *unified* picture of the structures found in  $\text{SmAP}_{Fmod}$ ,  $B_7$ , and  $\text{SmC}_{gmod}$  liquid crystals, without the need for any additional mechanisms. It is possible that by doping nearly rodlike molecules with chemical compatibility in BC compounds known to switch by a rotation around their long axes (as found in [35,36]), *bilayer* stripe phases with the structure shown in Fig. 12 may be *induced* by the nonpolar domains made of the rodlike molecules.

- 
- [1] P. G. de Gennes and J. Prost, *The Physics of Liquid Crystals* (Clarendon Press, Oxford, 1993).
- [2] A. S. Govind and N. V. Madhusudana, *Europhys. Lett.* **55**, 505 (2001).
- [3] N. V. Madhusudana, *Liq. Cryst.* **42**, 840 (2015).
- [4] H. Takezoe and A. Eremin, *Bent-Shaped Liquid Crystals* (CRC Press, Boca Raton Press, FL, 2017).
- [5] D. A. Coleman, J. Fernsler, N. Chattam, M. Nakata, Y. Takahashi, E. Korblova, D. R. Link, R. F. Shao, W. G. Jang, J. E. Maclennan, O. Mondainn-Monval, C. Boyer, W. Weissflog, G. Pelzl, L. C. Chien, J. Zasadsinski, J. Watanabe, D. M. Walba, H. Takezoe, and N. A. Clark, *Science* **301**, 1204 (2003).
- [6] N. V. Madhusudana, *Phys. Rev. E* **100**, 022706 (2019).
- [7] N. V. Madhusudana, *J. Phys.: Condens. Matter* **32**, 234003 (2020).
- [8] A. Jakli, D. Krueker, H. Sawade, and G. Heppke, *Phys. Rev. Lett.* **86**, 5715 (2001).
- [9] N. Chattham, E. Korblova, R. Shao, D. M. Walba, J. E. Maclennan, and N. A. Clark, *Phys. Rev. Lett.* **104**, 067801 (2010).
- [10] A. Roy, N. V. Madhusudana, P. Toledano, and A. M. Figueiredo Neto, *Phys. Rev. Lett.* **82**, 1466 (1999).
- [11] H. R. Brand, P. E. Cladis, and H. Pleiner, *Eur. Phys. J. B* **6**, 347 (1998).
- [12] C. Bailey and A. Jakli, *Phys. Rev. Lett.* **99**, 207801 (2007).
- [13] A. V. Emelyanenko and M. A. Osipov, *Phys. Rev. E* **70**, 021704 (2004).
- [14] N. Chattham, E. Korblova, R. Shao, D. M. Walba, J. E. Maclennan, and N. A. Clark, *Liq. Cryst.* **36**, 13092009.
- [15] N. Chattham *et al.*, *Phys. Rev. E* **91**, 030502(R) (2015).
- [16] J. P. Bedel, J. C. Rouillon, J. P. Marcerou, H. T. Nguyen, and M. F. Achard, *Phys. Rev. E* **69**, 061702 (2004).
- [17] E. Gorecka *et al.*, *J. Mater. Chem.* **18**, 3044 (2008).
- [18] A. Kovarova *et al.*, *Beilstein J. Org. Chem.* **10**, 794 (2014).
- [19] N. Vauptotic *et al.*, *Soft Matter* **5**, 2281 (2009).
- [20] C. Zhang *et al.*, *Liq. Cryst.* **39**, 1149 (2012).
- [21] W. H. Chen, W. T. Chuang, U. S. Jeng, H. S. Sheu, and H. C. Lin, *J. Am. Chem. Soc.* **133**, 15674 (2011).
- [22] I. H. Chiang, W. T. Chuang, C. L. Lu, M. T. Lee, and H. C. Lin, *Chem. Mater.* **27**, 4525 (2015).

- [23] N. V. Madhusudana, *Phys. Rev. E* **96**, 022710 (2017).
- [24] N. Vaupotic and M. Copic, *Phys. Rev. E* **72**, 031701 (2005).
- [25] N. Vaupotic, M. Copic, E. Gorecka, and D. Pocięcha, *Phys. Rev. Lett.* **98**, 247802 (2007).
- [26] C. Zhu *et al.*, *J. Am. Chem. Soc.* **134**, 9681 (2012).
- [27] D. Pocięcha, N. Vaupotic, E. Gorecka, J. Mieczkowski, and K. Gomola, *J. Mater. Chem.* **18**, 881 (2008).
- [28] A. Eremin, U. Kornek, R. Stannarius, W. Weissflog, H. Nadasi, F. Araoka, and H. Takezoe, *Phys. Rev. E* **88**, 062512 (2013).
- [29] R. Deb *et al.*, *J. Mater. Chem.* **20**, 7332 (2010).
- [30] A. Roy and N. V. Madhusudana, *Eur. Phys. J. E* **18**, 253 (2005).
- [31] D. Blankshtein and R. M. Hornreich, *Phys. Rev. B* **32**, 3214 (1985).
- [32] G. A. Hinshaw, Jr. and R. G. Petschek, *Phys. Rev. B* **37**, 2133 (1988).
- [33] A. E. Jacobs, G. Goldner, and D. Mukamel, *Phys. Rev. A* **45**, 5783 (1992).
- [34] M. Nakagawa, M. Ishikawa, and T. Akahane, *Jpn. J. Appl. Phys.* **27**, 456 (1988).
- [35] W. Weissflog *et al.*, *J. Mater. Chem.* **15**, 939 (2005).
- [36] M. Nakata, R. F. Shao, J. E. MacLennan, W. Weissflog, and N. A. Clark, *Phys. Rev. Lett.* **96**, 067802 (2006).
- [37] E. Gorecka *et al.*, *Chem. Phys. Chem.* **6**, 1087 (2005).
- [38] D. A. Coleman *et al.*, *Phys. Rev. E* **77**, 021703 (2008).
- [39] M. Manai *et al.*, *Ferroelectrics* **343**, 27 (2006).
- [40] N. A. Clark, D. Coleman, and J. E. MacLennan, *Liq. Cryst.* **27**, 985 (2000).